


Tunable friction performance of magneto-rheological elastomer induced by external magnetic field

Rui Li¹, Dejun Ren¹, Xiaojie Wang², Xiang Chen¹, Shiwei Chen³
and Xuan Wu²

Journal of Intelligent Material Systems
and Structures
1–11
© The Author(s) 2017
Reprints and permissions:
sagepub.co.uk/journalsPermissions.nav
DOI: 10.1177/1045389X17708043
journals.sagepub.com/home/jim


Abstract

In order to investigate the magnetic-induced friction properties of magneto-rheological elastomers, isotropic and anisotropic magneto-rheological elastomers are fabricated, tribological testing setup is built, and the friction experiment is carried out. The experimental results show that the isotropic magneto-rheological elastomer has a decreasing friction coefficient with magnetic field applied, which is also affected by particle volume fraction. The influence of magnetic field on friction coefficient of the anisotropic magneto-rheological elastomers is not monotonic. The experimental results also show that the friction coefficient of magneto-rheological elastomers decreases with the increase in load for both isotropic and anisotropic magneto-rheological elastomers in most circumstances. The volume fraction of carbonyl iron powders being around 10% is the best for magneto-rheological elastomers in tuning friction. The tunable range of friction could be as high as 25% under a magnetic field of 0.25 T. Images of the magneto-rheological elastomer interfaces show that the surface roughness is reduced by about 20.7% when a magnetic field of 0.5 T is applied. The aggregation phenomenon is observed on the surface of the magneto-rheological elastomer under a magnetic field. On the basis of three-dimensional surface topography, a preliminary model for the aggregation of micro asperities on the surface of the magneto-rheological elastomer is built to interpret the influence of the magnetic field on the tribological properties of magneto-rheological elastomers.

Keywords

tribology, magneto-rheological elastomer, magnetic field, roughness, aggregation phenomenon, experiment

Introduction

Friction occurs at the contacting surfaces of two encountering sliders. How to control friction has been a hot topic for centuries ever since the invention of machines in the human being's civilization. As the world is becoming more and more industrialized, tuning friction is becoming more and more important. The reasons generally lie in two aspects. On one hand, friction should be decreased for energy saving and reduction of wear of moving parts. According to statistics, nearly half of the world's energy is dissipated in friction, and wear due to friction accounts for 60% of the mechanical material failure (Scientific Data Sharing Platform of Advanced Manufacturing and Automation, 2015). On the other hand, friction should be increased for better locomotion and stability. It is well known that brakes, tires, grippers, and so on, function well only with enough friction. Besides, friction has been found to play an important role in biological adhesion systems. As has been clarified in the past decades, the

climbing ability of some typical animals, including the gecko and the tree frog (Autumn et al., 2000; Federle et al., 2006), is attributed to the interfacial forces between the fine and exquisite toe pad structure and substrates, for example, the van der Waal's forces between the micro/nano scale hairs and the substrate. The friction force is found more than just working in locomotion in the tangential direction with respect to the surface. It can also help control adhesion in the normal direction (Autumn et al., 2006; Wu et al.,

¹Chongqing University of Posts and Telecommunications, Chongqing, China

²Institute of Advanced Manufacturing Technology, Hefei Institutes of Physical Science, Chinese Academy of Sciences, Changzhou, China

³Chongqing University of Science and Technology, Chongqing, China

Corresponding author:

Xuan Wu, Institute of Advanced Manufacturing Technology, Hefei Institutes of Physical Science, Chinese Academy of Sciences, Changzhou 213164, Jiangsu, China.
Email: xwu@iamt.ac.cn

2015). Generally, increasing friction in the proper direction can enhance normal adhesive capacity, and vice versa. The animals produce strong attachment and easy detachment at will with this so-called “frictional adhesion.” Inspired by the wall-climbing animals, researchers have fabricated bioinspired adhesive arrays, which can be used in bioinspired wall-climbing robots, manipulators, bandages, and many other synthetic devices (Aksak et al., 2008). Hence, for better controlling of the attachment and detachment, locomotion enhancement, and load capability adjustment in these devices, it is natural that the emerging bioinspired adhesives has raised a potential yet important application of tunable friction.

Noticed and concerned ever since the civilization of human being, the friction’s origin has only been revealed for hundreds of years. Interfacial effects including mechanical interlocking, capillary forces, van der Waal’s force, chemical bounds, and so on, all make contributions to the friction at different scales (Delrio et al., 2012). Factors both including loads and the surface’s property affect the weights of the different interfacial effects. Tuning friction has been technically realized by many methods, including adjusting normal forces, surface patterning, and lubrication (Bi, 2001; Xiao et al., 2012; Zhang et al., 2014). But they all have disadvantages. For example, when there is no pressing force, the normal force cannot enhance the friction. Surface patterning is not adaptable and easy to be worn down. Lubrication causes contamination. Therefore, external stimuli-induced friction control is necessary for the bioinspired adhesive technology. Is there a way that friction can be tuned as will without the mentioned disadvantage?

The magneto-rheological elastomer (MRE), whose stiffness and interfacial property are controllable under external magnetic field (Koo et al., 2010), provides a possible solution, and related research has been carried out. Lee et al. (2012) took the approach of observing the microstructure of the MRE filled with Fe, Ni, and Co powders in external magnetic field. They found that the carbonyl iron powders (CIPs) assembled to form larger particles and proposed that this phenomenon might lead to the change of the effective elastic modulus, which consequentially alter the tribological properties of the MRE. In addition, the frictional coefficients of MRE with/without the magnetic field were tested, and the stick-slippery phenomenon was found, which was influenced by the magnetic field and the velocity. Lian et al. (2015) studied the influence of the matrix materials on the MRE’s friction and wear behavior by fabricating MREs with four different matrices. By testing the hardness and wear with/without magnetic field, it was found that the polyurethane (PU) wrapped in silicone rubber exhibited the strongest resistance to wear. In addition, vibration (Lian et al., 2016) is also one of the factors that affect the friction performance. The friction coefficient increases with increasing

frequency and decreases with increasing amplitude of the vibration.

Previous study focused on the observation and interpretation of experimental results of the MRE’s tunable tribological properties, with basic mechanism proposed and influences of some of the MRE’s internal/external factors clarified. However, how the magnetic field influences the friction coefficient of MREs with different internal structures has not been studied. The changes of the MRE’s friction coefficient under certain magnetic field cannot be predicted, yet. Moreover, the interfacial effect of the MRE with/without external magnetic field has not been systematically investigated, and the origin of the tunable MRE’s tribological properties has not been analyzed. An understanding of the MRE’s tunable friction properties from a multi-scale perspective is, in fact, the very fundamental mechanism of this study. The development and potential applications of the MRE as for the synthetic smart adhesives are limited by these unknown mechanism.

In this article, we carry out tribological experiments of the MRE to study the controllable frictional property in quasi-static stick-slippery motions. The influence of internal factors such as MRE components of particle volume fractions and structures as well as external factors such as normal forces on the friction coefficients is studied. Interfacial images of MRE are taken to investigate the interfacial feature with and without external magnetic field. Finally, a preliminary model is established to explain how the magnetic fields induce the changes of friction coefficient of MREs.

Materials and methods

Fabrication of the samples

In the experiment, we fabricated isotropic and anisotropic MRE samples. The isotropic MRE samples, in which the CIPs are randomly distributed, were fabricated using silicon rubber (HT-18; Shanghai Tongshuai Co., Ltd, China) as matrix, with a volume ratio of 100:5 between Part A and B. The filler is CIP (Beijing Xing Rong Yuan Technology Co., Ltd., China) whose diameter is 5 μm . We also used polydimethylsiloxane (PDMS; 50 cp two methyl silicone oil; Dow Corning, USA) as diluting agent and KH570 ($\text{Y}(\text{CH}_2)_n\text{SiX}_3(\text{KH570})$) as silane coupling agent. Before the fabrication, we first diluted the Part A of the silicon rubber using diluting agent, as it is too viscous. We then pre-treated the CIPs using KH570, to help the CIPs build stronger chemical boundary with the silicon rubber. The samples were fabricated after the pre-treatment, by mixing the CIP and Part A and dispersing them by ultrasonic, and then mixing them with silicone rubber Part B, followed by stirring and air bubble removing in vacuum, and curing under room temperature. We prepared four samples in which the

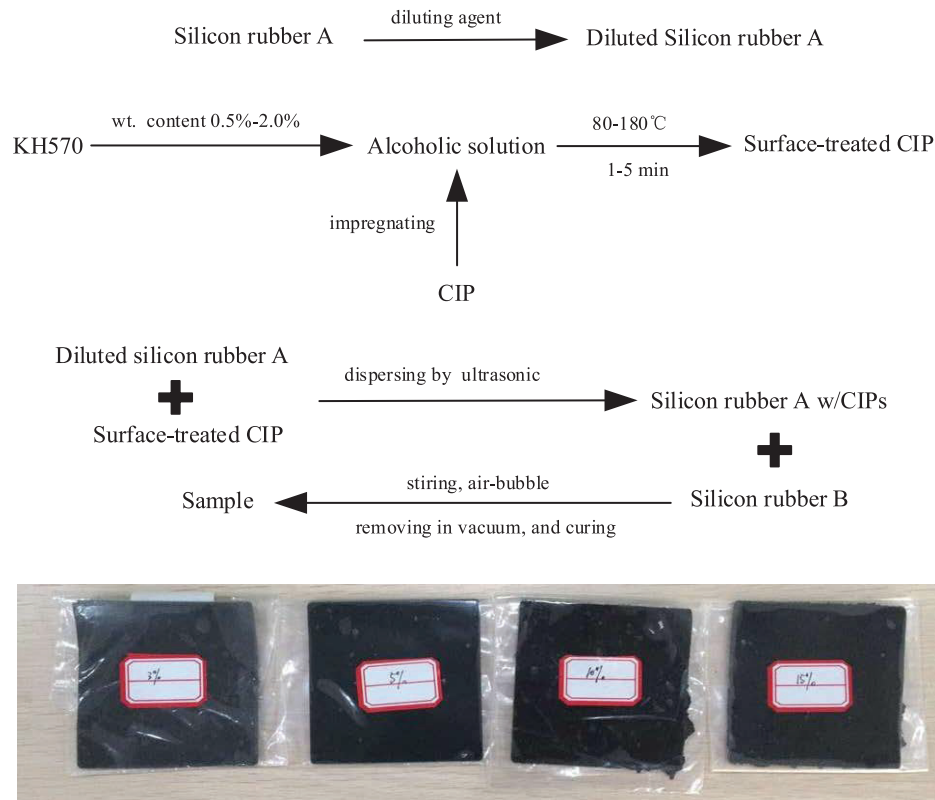


Figure 1. The flow chart of preparing isotropic MRE and samples.

CIP's content ratio varied from 3% to 15%, in terms of volume. The flow chart of the preparation and the samples is shown in Figure 1.

In the fabrication of the anisotropic MREs, 107 silicon rubber (Shanghai Silicon Polymer Materials Co., Ltd, China), which contained only one part, was selected as the matrix. The fillers were the same as those of the isotropic MREs. Crosslinking agent (tetraethoxysilane) and catalyst (dibutyltin dilaurate; Shanghai Silicon Polymer Materials Co., Ltd) were used in making the anisotropic MREs. Due to the low viscosity of the 107 silicone rubber, the CIPs were directly mixed with the liquid rubber. The mixture was then dispersed using the ultrasonic, mixed with crosslinking agent and catalyst, and stirred, followed by air-bubble-removing in the vacuum. Finally, it was stored in an external magnetic field as high as 0.8 T to cure, during which CIPs aligned in the magnetic field's direction to form chains. The procedure and the samples are shown in Figure 2. All MRE samples are cuboid-like with the dimension of 55 mm × 30 mm × 2 mm. All samples were numbered to identify different volume fractions of the CIPs, as listed in Table 1.

Test platforms

We carried out the experimental study to investigate the friction mechanism of MREs under the effect of an

applied magnetic field; therefore, it is necessary to test the magnet-induced friction coefficient and observe the interface of the MRE. For these purposes, two different platforms were established including the tribological testing apparatus and the interfacial observing platform, both of which equipped with a permanent magnet.

Tribological testing setup. The schematic of the tribological testing setup is shown in Figure 3. The slider is pressed to the MRE by a constant normal force, dragged along the surface, and the friction coefficient is obtained using the formula $f = F/W$, where F is the friction force and W is the normal force. The MRE is fixed on the magnet holder, which holds a permanent magnet.

A customized apparatus for the friction testing has been built as shown in Figure 4. The apparatus includes two linear stages, two sensors, one slider, and one magnet holder. The two linear stages (T-LSM200B and T-LSM050B; Zaber Technologies Inc., Canada) output linear motions in two orthogonal axes, which are parallel and vertical to the testing surface of the MRE, namely, the horizontal and vertical axis, respectively, or x - and y -axis. The two sensors (LSM300 and LSM250; FUTEK Advanced Sensor Technology, Inc., USA), connected to the y -axis stage, detect the contact forces in two directions, which are friction and normal forces, respectively. The slider is fixed with the sensor for

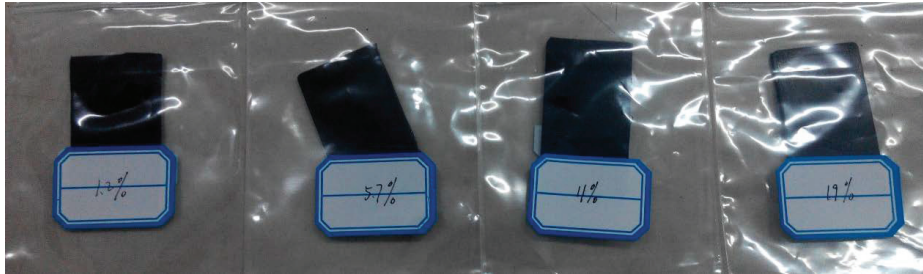
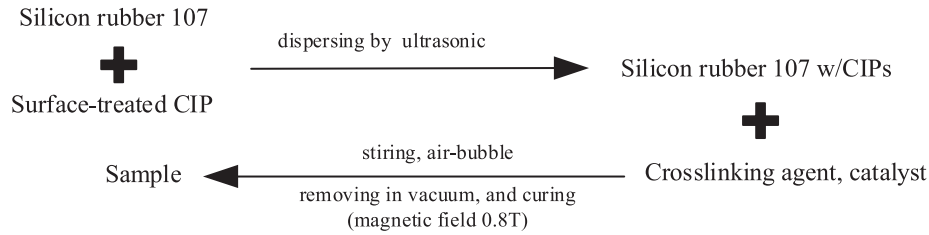


Figure 2. The flow chart of preparing anisotropic MRE and samples.

Table 1. Test samples.

Test sample	Sample number	The volume fraction of CIPs (%)
Isotropic MRE	1	3
	2	5
	3	10
	4	15
Anisotropic MRE (0.8 T)	5	1.2
	6	5.7
	7	11
	8	19

CIPs: carbonyl iron powders; MRE: magneto-rheological elastomer.

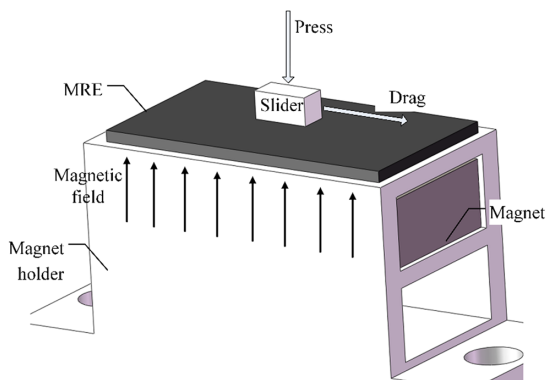


Figure 3. The schematic of experimental setup for friction test.

normal force measurement, which contacts the testing surface of the MRE samples. The size of contact area is $10 \text{ mm} \times 5 \text{ mm}$. A high-strength neodymium magnet

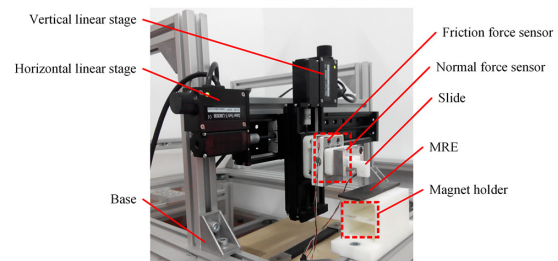


Figure 4. The tribological test apparatus.

is put into the magnet holder, providing magnetic field as high as 0.25 T at the surface of testing samples during experiment.

Interfacial observing setup. Under the condition of dry friction, the interface morphology of the MRE is one of the main factors that affect the friction performance. Observation of the MRE interface before and after applied magnetic field could directly determine whether the interface is affected by the magnetic field. The schematic of the observation setup is shown in Figure 5. A metallographic microscope (ZEISS AXIOVERT 200 MAT) is employed to obtain the two-dimensional morphology of MRE. A permanent magnet is installed right below the MRE, which could produce a magnetic field as high as 0.25 T at the observed interface. A white light interferometer (ContourGT-K) is applied to obtain the three-dimensional (3D) morphology of MRE samples, including surface topography, roughness, peaks and valleys. Another permanent magnet is also installed right below the MRE when taking the

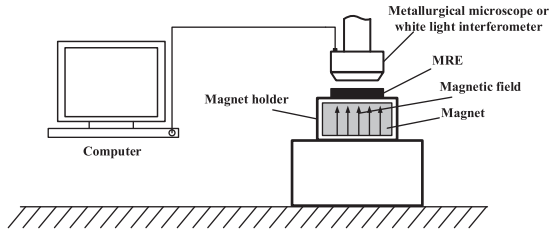


Figure 5. Schematic of optical surface observation setup.

image pictures. The magnet could produce a magnetic field as high as 0.5 T at the observing interface. A PC is connected to the optical instruments to store and process the image data.

Testing procedure

Tribological testing. The test procedure is designed as follows: the vertical stage first presses the sample, and then the horizontal stage drags the sample. The force data in the stick-slip process are acquired by the sensors, recorded by the oscilloscope, and at last filtered and stored in the PC. In order to remove the impurities (dirt, grease, etc.) on the interface of the sample, which could affect the experimental results, alcohol is used to wipe the surface of the MRE, followed by each test after the surface moisture is evaporated. The relative sliding velocity between the friction pairs is $10 \mu\text{m/s}$.

Interface observation. Sample no. 2 was chosen as the object of the surface observation. In the observation, the sample's interface was cleaned using alcohol in the way presented in section "Tribological testing." It was first observed without applied magnetic field and then pictured the surface under a magnetic field. Images of the interface were collected and processed in PC.

Results

Tribological testing

The raw data of the normal force and the friction force are shown in Figure 6. These data were transferred into force signals according to the sensors' force–voltage relationship. As can be seen from Figure 6, in the whole test processing, the raw data of the normal force in the vertical direction basically remain constant, indicating that the setup is stable. Key points are marked in the figures as A, B, and C. The vertical stage presses the sample at A, the horizontal stage drags the sample from B to C, and at C the stick-slip process begins. The friction coefficients which are the values of friction force divided by normal force are computed using the data in the regime after C.

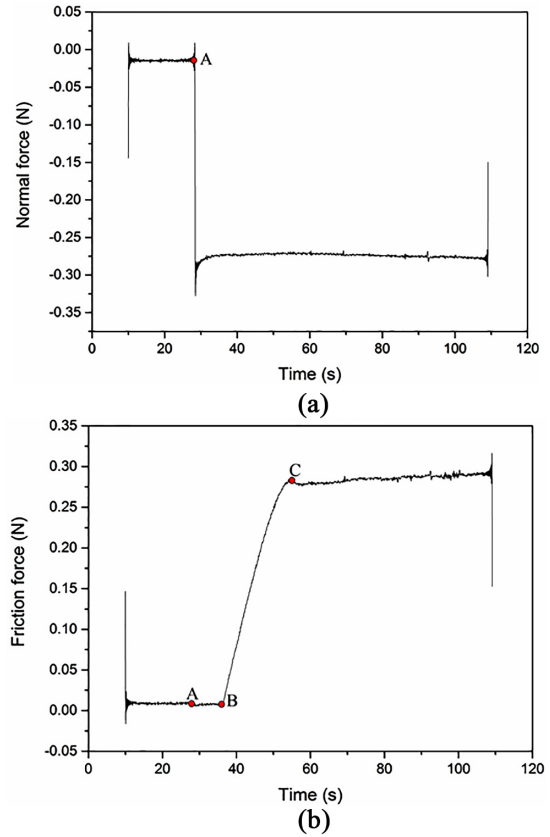


Figure 6. Raw data of the friction measurement process: (a) raw data of the normal force and (b) raw data of the friction force.

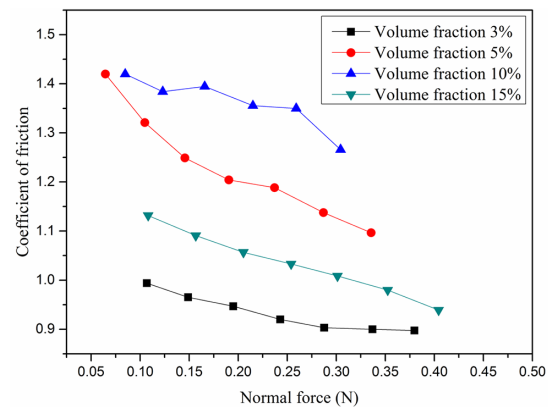


Figure 7. The friction coefficients of isotropic MREs with respect to normal force (magnetic field OFF).

Tribological experiment results

In Figures 7 and 8, we illustrate the experimental results of the friction coefficients of the isotropic and anisotropic MREs with respect to normal forces, respectively, under zero magnetic fields. As can be seen, the friction coefficients of the MREs decrease as the normal forces increase, except for the anisotropic MRE

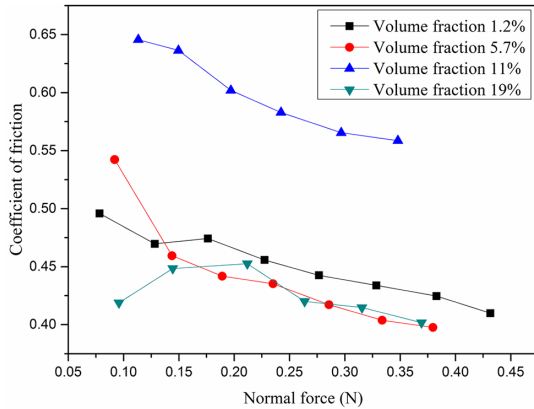


Figure 8. The friction coefficients of anisotropic MREs with respect to normal force (magnetic field OFF).

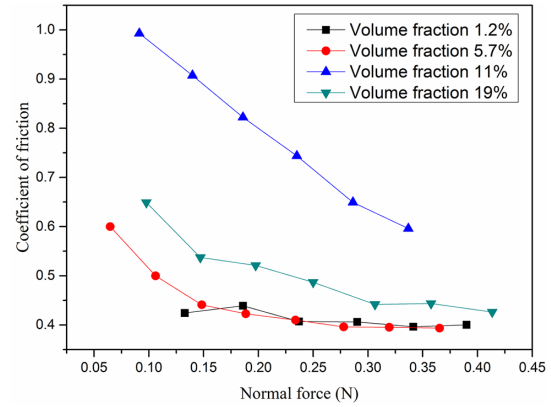


Figure 10. The friction coefficient of MRE anisotropic change with normal force (magnetic field ON, 0.25 T).

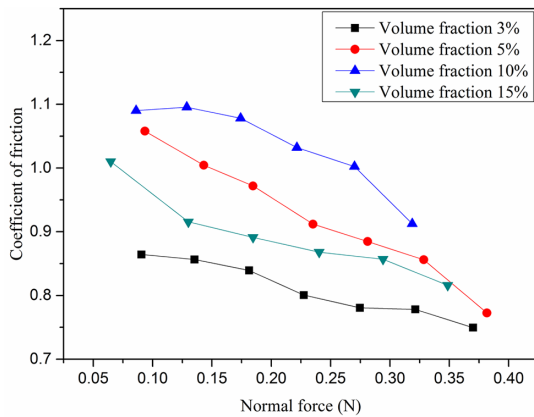


Figure 9. The friction coefficient of MRE isotropic change with normal force (magnetic field ON, 0.25 T).

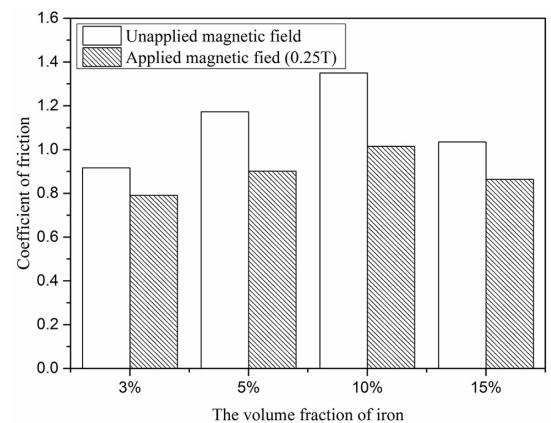


Figure 11. Friction coefficient of isotropic MRE with different volume fractions under 0.25 N.

with particle volume fraction of 19%, which shows an increase and decrease with normal forces. All the testing results shown in Figures 7 and 8 demonstrate that the friction coefficients of MREs vary with particle volume fractions.

Figures 9 and 10 illustrate the experimental results of the friction coefficients of the isotropic and anisotropic MREs with respect to normal forces, respectively, with an applied magnetic field. It can be seen that the friction coefficients of the MREs monotonically decrease as the normal forces increase except for the sample of CIP's volume fraction of 1.2%. The friction coefficients also vary with different volume fractions both with and without external magnetic field. From tribological experiment, we find that nearly all of the friction coefficients of the MREs monotonically decrease as the normal forces increase. That is because adhesion-induced friction is the main factor during sliding friction, and we will discuss this problem in detail in section "Effect of normal force on the MRE magnetic friction properties."

From previous experimental results, we can see that normal force is one of the factors affecting the friction coefficient. In order to investigate the influence of the CIP's volume fraction and magnetic field on the friction coefficients of the isotropic and anisotropic MREs, the normal force should be set to constant value. We choose middle value of normal force of 0.25 N in our tests and show the friction coefficients of isotropic and anisotropic MRE with respect to the CIP's volume fraction. The comparisons of the results with/without applied magnetic fields are shown in Figures 11 and 12, respectively. As can be seen, the friction coefficients of isotropic MRE are reduced by an applied magnetic field. However, for the anisotropic MREs, the magnetic field affecting the friction coefficient changes depends on the particle volume fraction of the testing samples. The experimental results also show that with the same normal force, the friction coefficient varies with the CIP's portion inside the MREs. An optimal fraction of particles exists for the largest relative changes of the friction coefficients under a magnetic field. In this

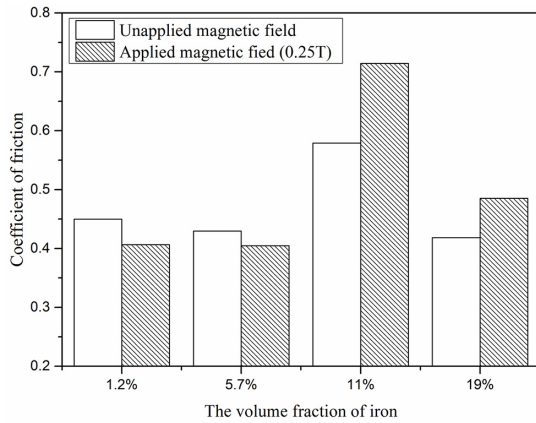


Figure 12. Friction coefficient of anisotropic MRE with different volume fractions under 0.25 N.

study, we found that the CIP's volume fraction being around 10% is the best for MREs in tuning friction. The tunable range of friction could be as high as 25% under a magnetic field of 0.25 T.

Interfacial observation results

Figure 13(a) and (b) is the interfacial image taken after gray processing without and with magnetic field under metallographic microscope, respectively. Figure 13(c) and (d) is the image which was processed using two-value algorithm. In the two-value image, the location of

CIPs can be spotted, and in the gray image, the size and the distribution of the particles can be obtained. We compared the two-value images with corresponding gray images. By the comparison, we found that the microstructure of the interface is changed after the magnetic field is applied. From Figure 13(a) and (c), it can be seen that without applying a magnetic field, the particles are more scattered, and the degree of aggregation of ferromagnetic particles is low. In Figure 13(b) and (d), however, smaller particles are assembled to form larger particles, while the total number of larger particles is increased and the aggregation degree is increased. It confirms that the magnetic field causes the surface particle aggregations of MREs.

The 3D morphology of the MRE interface obtained by the white light interferometer is shown in Figure 14. From Figure 14, the micro/nano scale microstructures of MREs' surface are clear. It can be seen that the part of red is the peaks, and the part of blue is the valleys. Figure 15 shows the peaks and valleys of the MRE interface at the micro/nano scale in the form of two-dimensional contour lines. The surface roughness is $2.5198 \mu\text{m}$ under zero magnetic field, while it is $1.9984 \mu\text{m}$ under a magnetic field of 0.5 T. The results show that with a magnetic field of 0.5 T, the surface roughness of MRE is reduced by about 20.7%. There are a lot of peaks and valleys on the surface of MRE. The surface roughness of MRE has changed just because of CIPs' aggregation with magnet field, and we will discuss this problem in detail in section "Effect of

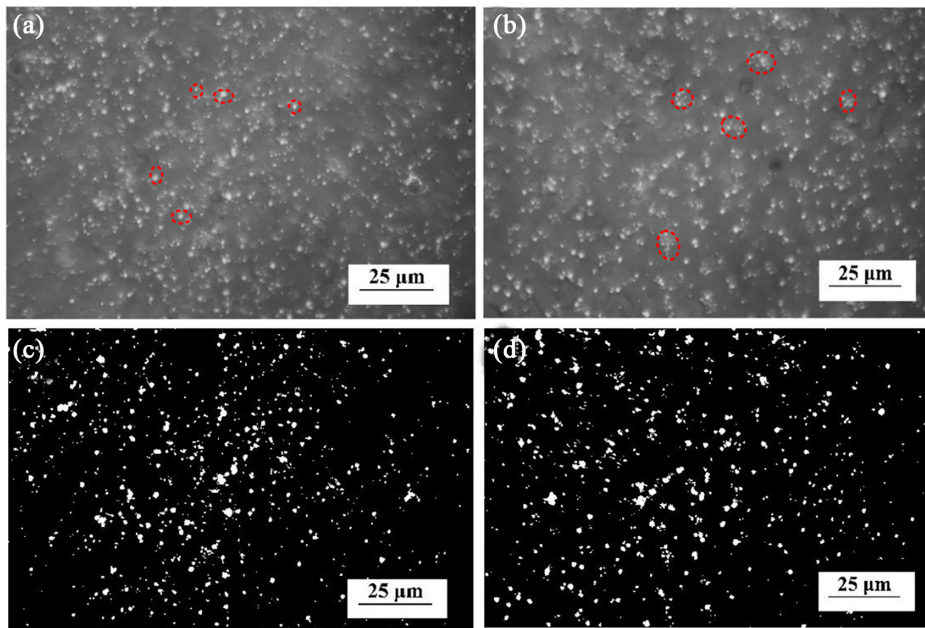


Figure 13. Surface microstructure of MRE (a, c) without magnetic field and (b, d) with magnetic field; the magnetic field intensity is 0.25 T. The figure includes (a, b) gray image and (c, d) two-value image. (a, b) In the gray image, the ferromagnetic particles before applied magnetic field and corresponding aggregation of these particles after applied magnetic field are marked with red circle. (c, d) In the two-value image, the black part is rubber, and the white spot is the iron magnetic particle.

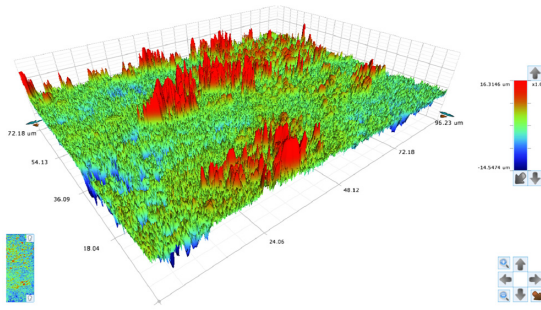


Figure 14. Three-dimensional contour surface of MRE. The red color shows the area of CIPs' aggregation or larger groups of CIPs.

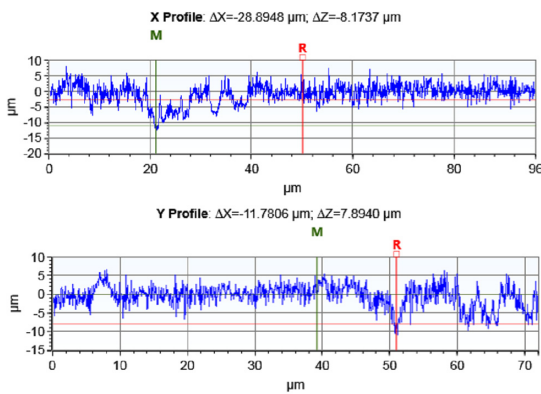


Figure 15. Two-dimensional contour surface of MRE.

magnetic particles aggregation on the magnetic friction properties.”

Discussions

In previous section, we experimentally show that the friction coefficients of both isotropic and anisotropic MREs are affected by the factors of the normal force, magnetic field, and the CIP's volume fraction. It means that, given switchable external magnetic field and variable normal forces, the MRE's tribological properties can be tuned even if the internal factors are constant. Therefore, how the external factors affect the MRE's friction coefficient is the key to understand the in-depth mechanism. In the following, we will discuss and analyze the phenomena.

Effect of normal force on the MRE magnetic friction properties

In the course of the experiments, the normal force range is between 0.05 and 0.5 N, which could be categorized as small loadings. The experimental results show that in most circumstances the friction coefficients of both

isotropic and anisotropic MREs decrease with increasing normal force. Taking into account that the rubber is the main component of MREs, we borrowed related friction theorem of the rubber materials (Wang, 2000; Zhou et al., 2013) to explain the phenomenon. Assuming the elastomer is viscoelastic when encountering solid slider under light loadings. Therefore, a two-term model of the friction force, in which the adhesion-induced friction between the elastic body and the nylon surface, and the hysteresis resistance force of the rubber, acting together presents apparent friction forces of MREs. The former term brings in a part of the friction force in which the coefficient is inversely proportional to the normal force, and the latter brings into one that is negligible with increasing normal force. Therefore, the results show that the friction coefficient decreases with the increase in the normal force, which is consistent with the experimental measurements.

Effect of magnetic particle aggregation on the magnetic friction properties

The two-term formula of the friction force F of the MRE can be expressed as

$$F = \alpha A + \beta W = \beta \left(\frac{\alpha}{\beta} A + W \right) \quad (1)$$

which considers the friction as the sum of the molecular force (αA) and mechanical interactions (βW) between the surface asperities. A is the contact area, while α and β are regarded as constants related to the materials and profiles of the contacting surfaces (Wen and Huang, 2012). Consequentially, we have the equivalent friction coefficient on the surface of the single MRE asperity

$$f = \frac{\alpha A}{W} + \beta \quad (2)$$

In the experiment, the isotropic MREs' frictional coefficient decreases with an applied magnetic field for all the MRE samples with various CIPs' volume fractions, while the frictional coefficient of anisotropic MRE does not, which depends on the CIPs' volume fractions. The inner CIPs' chain structure might be the reason for the uncertainty. Here, we focus on the governing law of the isotropic MREs, as the inner fillers' distribution is rather uniform and managed to build a mathematical model of the contact on the interface. As can be seen from the MRE surface, it does have a lot of micro asperities and valleys. The surface roughness is composed of such asperities and valleys. Figure 16 shows part of the MRE's interfacial profile. When encountering the rigid, flat surface, the rough peak on the MRE interface can be approximately regarded as the contact area of the body, and the radius of the curvature could be regarded as a constant, to make the

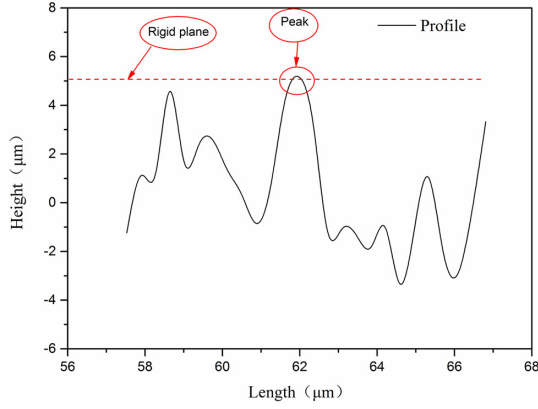


Figure 16. Two-dimensional topography of the vertical direction of the magnetic rheological elastomer.

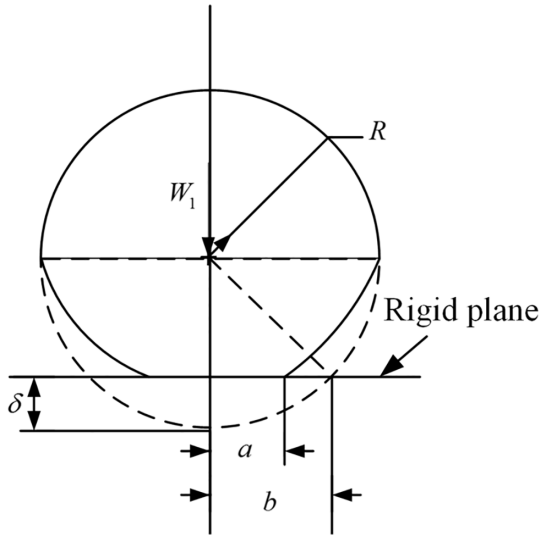


Figure 17. Single peak elastic contact model. The dotted line refers to the undeformed profile and the solid line refers to the deformed profile of the sphere.

rough peak part of a sphere, with bulk elastic modulus of MRE as E and the radius as R , as shown in Figure 17. Furthermore, the equivalent contact model of two spheres can be simplified as the contact between a sphere with elastic modulus E' and radius R and a rigid, flat plane. Hence, using the Hertz Contact model (Johnson, 1985) we have

$$\delta_1 = \left(\frac{9W_1^2}{16E'^2R_1} \right)^{1/3} \quad (3)$$

$$a_1 = \left(\frac{3W_1R_1}{4E'} \right)^{1/3} \quad (4)$$

$$W_1 = \frac{4}{3}E'R_1^{1/2}\delta_1^{3/2} \quad (5)$$



Figure 18. Hypothetical MRE surface.

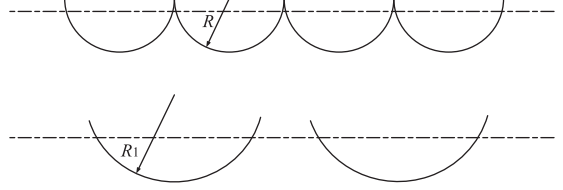


Figure 19. Aggregation model where the two peaks aggregated into one.

where W_1 is the local normal force applied to a single asperity, δ_1 is the normal deformation, and a_1 is the radius of the contact circle area. Simplifying the formula can help obtain that

$$a_1^2 = R_1\delta_1$$

Thus, the actual contact area A_1 of the single micro asperity on the surface of the MRE shown in Figure 17 is

$$A_1 = \pi a_1^2 = \pi R_1\delta_1 \quad (6)$$

and the volume of the single micro-asperity is

$$V_1 = \frac{4}{3}\pi R_1^3 \quad (7)$$

Suppose that the original surface of the MRE has n rough peaks of the same dimension (Figure 18), with uniform deformation, and the total actual contact area of the micro asperities of the MRE surface is $A = nA_1$.

In the experiment, we observed that under constant normal force, the magnetic field reduced the friction coefficient of the MRE surface. Equation (2) indicates that the actual contact area A might have directly resulted in the change of friction coefficient f . This is possibly caused by the aggregation of adjacent asperities, which is the consequence of their alignment to form chains within the MRE bulk. Considering the situation in which the aggregation occurs between two adjacent asperities of the same dimensions, with no gap between the asperities or volume changes, and no longitudinal variation (Figure 19), we have

$$2\frac{4}{3}\pi R_1^3 = \frac{4}{3}\pi R_2^3 \quad (8)$$

where R_2 is the radius of the single micro asperity after aggregation. It can be simplified that

$$R_2 = 2^{1/3}R_1 \quad (9)$$

Using equations (3) to (6), the total actual contact area of the two asperities after aggregation could be written as

$$A_2 = 2^{1/3} \pi R_1 \delta_1 \quad (10)$$

while the actual contact area of the two individual MRE micro asperity peaks before the aggregation is

$$2A_1 = 2\pi R_1 \delta_1 \quad (11)$$

From equations (10) and (11), it can be seen that the actual contact area of the two MRE surface micro asperity bodies is smaller than the actual contact area before the aggregation.

In fact, when two or more asperities aggregate in magnetic field, the actual contact area will be reduced. The total actual contact area of the aggregation could be written as

$$A' = 2^{1/3} m \pi R_1 \delta_1 + 3^{1/3} k \pi R_1 \delta_1 + \dots \quad (12)$$

In equation (12), m is the number of cases in which two micro asperities on the MRE surface aggregate, k is the number of cases in which three micro asperities on the MRE surface aggregate, and $n = 2m + 3k + \dots$. Thus, we have that

$$n \pi R_1 \delta_1 > A' = 2^{1/3} m \pi R_1 \delta_1 + 3^{1/3} k \pi R_1 \delta_1 + \dots \quad (13)$$

By inequality (13), we can know that when the magnetic field is applied, the MRE surface micro asperities tend to aggregate and the actual contact area becomes smaller, which leads to the decrease in the friction coefficient of the MRE surface. This has been verified by the two-dimensional surface observation experiments (Figure 13), as aggregation can be observed as the particles diameters increase.

Conclusion

1. The tribological properties of the isotropic MRE could be controlled by magnetic field. The magnetic field could change the surface morphology (roughness), elastic modulus, and some other factors, which consequentially affect the interfacial properties of the MRE. With the increase in the volume fraction of the CIP, the friction coefficient also varies under a constant magnetic field. The experimental results show that the friction coefficient's relative change of MREs with the CIP's volume fraction of 10% can reach as high as 25% when a magnetic field of 0.25 T is applied.
2. As for the anisotropic MRE, the experimental results show that the magnetic field has an effect on the change of tribological performance, but

the trend is not monotonic. Due to the chain structure of the material, in the presence of the magnetic field, the friction coefficient of MRE varies with uncertainty.

3. The experimental results show that under the external magnetic field, the surface roughness of MRE is reduced by about 20.7%. Besides, under the external magnetic field, the aggregation of MRE surface micro asperities occurs. Those factors can lead to the decrease in friction coefficient of MRE surface. The theoretical model agrees well with the experimental results, which can be used to explain why the MRE magnetic-induced tribological properties can be controlled. The results show that the application of the MRE in tunable tribological properties is promising.
4. Under light loadings, the friction force mainly origin from the adhesion. In most circumstances, the friction coefficients of both isotropic and anisotropic MRE decrease as the normal load increases.

Declaration of conflicting interests

The author(s) declared no potential conflicts of interest with respect to the research, authorship, and/or publication of this article.

Funding

The author(s) disclosed receipt of the following financial support for the research, authorship, and/or publication of this article: This work was supported by Chongqing Science Foundation for Distinguished Young Scholars (cstc2014jcyj40004), the National Nature Science Foundation of People's Republic of China (Projects No.11372366, No. 51605467), and Chongqing Postgraduate Research and Innovation Project (CYS16160).

References

- Aksak B, Murphy MP and Sitti M (2008) Gecko inspired micro-fibrillar adhesives for wall climbing robots on micro/nanoscale rough surfaces. In: *IEEE international conference on robotics and automation*, Pasadena, CA, 19–23 May, pp. 3058–3063. New York: IEEE.
- Autumn K, Dittmore A, Santos D, et al. (2006) Frictional adhesion: a new angle gecko attachment. *Journal of Experimental Biology* 209: 3569–3579.
- Autumn K, Liang YA, Hsieh ST, et al. (2000) Adhesive force of a single gecko foot-hair. *Nature* 405(6787): 681–685.
- Bi LY (2001) Integrated approach to change the rubber friction properties. *World Rubber Industry* 28(1): 36–39 (in Chinese).
- Delrio FW, Dunn ML and Boer MPD (2012) Van der Waals and capillary adhesion of polycrystalline silicon micromachined surfaces. In: Bhushan B (ed.) *Scanning Probe Microscopy in Nanoscience and Nanotechnology* 3. Berlin, Heidelberg: Springer, pp. 363–393.

- Federle W, Barnes W, Baumgartner W, et al. (2006) Wet but not slippery: boundary friction in tree frog adhesive toe pads. *Journal of the Royal Society Interface* 3(10): 689–697.
- Johnson KL (1985) *Contact Mechanics*. London, UK: Cambridge University Press.
- Koo JH, Khan F, Jang DD, et al. (2010) Dynamic characterization and modeling of magneto-rheological elastomers under compressive loadings. *Smart Materials and Structures* 19(11): 117002.
- Lee DW, Lee KH, Lee CH, et al. (2012) A study on the tribological characteristics of a magneto-rheological elastomer. *Journal of Tribology* 135(1): 014501.
- Lian C, Lee KH and Lee CH (2015) Friction and wear characteristics of magneto-rheological elastomers based on silicone/polyurethane hybrid. *Journal of Tribology* 137(3): 031607.
- Lian C, Lee KH and Lee CH (2016) Friction and wear characteristics of magnetorheological elastomer under vibration conditions. *Tribology International* 98: 292–298.
- Scientific Data Sharing Platform of Advanced Manufacturing and Automation (2015) Available at: http://www.amadata-net.cn/design_tech/design_mcjs.aspx (accessed 1 July 2016).
- Wang GY (2000) Friction and testing of rubbers. *Special Purpose Rubber Products* 3: 55–62 (in Chinese).
- Wen SZ and Huang P (2012) *Principles of Tribology*. Beijing, China: Tsinghua University Press Ltd (in Chinese).
- Wu X, Wang X, Mei T, et al. (2015) Mechanical analyses on the digital behaviour of the Tokay gecko (Gekko gecko) based on a multi-level directional adhesion model. *Proceedings of the Royal Society A* 471(2179): 20150085.
- Xiao Q, Lin FG, Wang CG, et al. (2012) Analysis on wheel-rail rolling contact characteristics with variable friction coefficient. *Journal of the China Railway Society* 34(6): 24–28 (in Chinese).
- Zhang YS, Mi XM, Yu YL, et al. (2014) Structural improvements for reducing friction in pneumatic cylinder. *Journal of Lanzhou University of Technology* 40(2): 55–59 (in Chinese).
- Zhou GW, Wang JX, Li JY, et al. (2013) Experimental investigation of tribological properties for spiral groove water lubricated rubber bearings. *Journal of Chongqing University* 36(03): 1–5 (in Chinese).